Extraction of Temperature Distribution Using Deep Neural Networks for BOTDA Sensing System

Biwei Wang[1], Nan Guo[1], Faisal Nadeem Khan[1], Abul Kalam Azad[1], Liang Wang[2, *], Changyuan Yu[1] and Chao Lu[1]

[1]Department of Electronic and Information Engineering, The Hong Kong Polytechnic University, Kowloon, Hong Kong SAR, China.

[2]Department of Electronic Engineering, The Chinese University of Hong Kong, NT, Hong Kong SAR, China.

[*]lwang@ee.cuhk.edu.hk

***Abstract*—Extraction of temperature distribution using the method of deep neural networks (DNN) for Brillouin optical time domain analyzer (BOTDA) system is demonstrated experimentally. After appropriate training of DNN model, temperature distribution information along the fiber under test could be directly extracted from the experimentally obtained local Brillouin gain spectrums (BGS) using DNN without the need of calculating Brillouin frequency shift (BFS) and transforming it to temperature as conventional Lorentz curve fitting (LCF) method does. The results of Temperature extraction using DNN show comparable accuracy to that of using conventional LCF method.**

Keywords—Temperature extraction; Brillouin optical time domain analyzer (BOTDA); Deep neural networks (DNN).

I. Introduction

Since the Brillouin optical time domain analyzer (BOTDA) was proposed by T. Horiguchi and M. Tateda for the first time in 1989 [1], BOTDA has been a very hot research direction as a method of distributed fiber optic sensors. Many research works have been reported in this field in the past twenty years and high spatial resolution and long measurement distance BOTDA systems for temperature\strain measurement have been achieved [2-7]. The BOTDA sensing system is based on the fundamental principle that the pump pulse light will transmit its power to the counter propagating continuous wave known as probe light under the stimulated Brillouin scattering (SBS) effect if the frequency difference between them is around the Brillouin frequency shift (BFS). Since the local change of BFS is proportional to the local temperature or strain change, the temperature or strain distribution information along the fiber under test (FUT) could be obtained from the BFS distribution. And the local BFSs are conventionally determined by the central frequency of local Brillouin gain spectrums (BGSs), which could be obtained by sweeping frequency offset of the interacting light waves around the BFS and using the conventional curve fitting technique, e.g. Lorentz curve fitting (LCF) method to process the experimental data. The spatial information could be extracted as well because the pump pulse and the probe are interacting in different location along the FUT.

On the other hand, the deep neural networks (DNN) as a type of deep learning methods in machine learning field is a very hot research topic in recent years and it has been widely used in the field of speech recognition [8-10] and also in fiber optical communication, e.g. modulation format identification [11]. Compared with the artificial neural network (ANN), the DNN is easier to construct and train, as it can learn rich features automatically through a supervised or unsupervised feature learning process, while the use of ANN needs specifically designed structure, especially when the relation between targeted output and input is complex and the number of layers between output layer and input layer is required to be large. Recently, our group has demonstrated temperature extraction using ANN for BOTDA sensing system [12], indicating advantages of using ANN for temperature extraction over conventional curve fitting techniques. Since DNN is easier for both training and testing phase, here we propose to use DNN instead of ANN in extracting the temperature distribution information directly from the local BGSs along the FUT for our BOTDA system. The principle of this method is that the DNN could inherently represent a non-linear relation between the BGS and the temperature after appropriate training process. In this paper, the extraction of temperature distribution using DNN with comparable accuracy to conventional LCF is achieved.

II. Principle and Experiment Setup

A. Principle of DNN

DNN is a computer processing model to simulate the learning process of human brains, in which information is transmitted and processed by many neurons parallelly and layer by layer. The DNN structure with two autoencoder hidden layers is shown in Fig. 1. The DNN is constructed of one input layer, some hidden layers and one output layer. The output of each neuron in the hidden layers or output layer could be represented using an activation function:

$$y_j = f_j\left(\Sigma_i\, w_{ij}\, x_i - \theta_j\right). \tag{1}$$

Here y_j is the output of the j^{th} node, x_i is the i^{th} input to the node, w_{ij} is the adjustable weight connecting the input node i

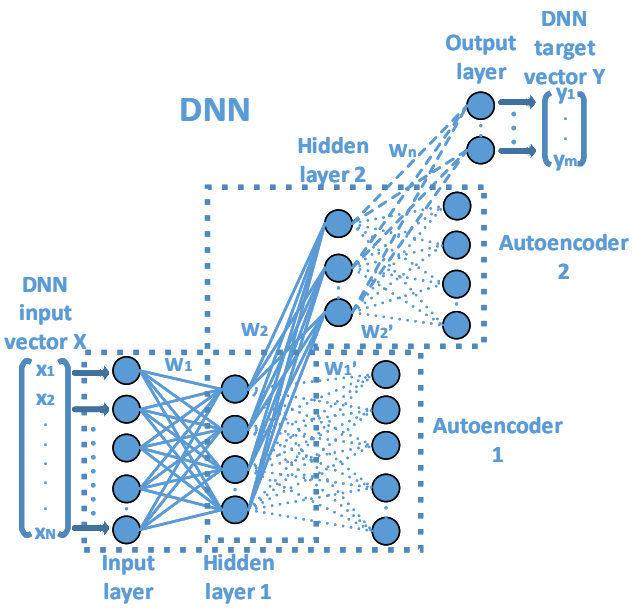

Fig. 1. The structure of DNN with 2 autoencoder hidden layers.

and the output node j, θ_j is the threshold of the j^{th} node and f_j is a nonlinear activation function. From this equation, we could see that the output of each neuron has a linear relation with all neurons in the prior one layer. So the output of each neuron in the final output layer of this model has a nonlinear relation with the initial input vector, since there is one or more hidden layers between the input layer and the output layer. The number of neurons in each hidden layer usually reduces gradually and the hidden layer functions as feature extractor in fact.

The utilization of DNN contains two stages: training and testing. In the training stage, firstly each hidden layer and final output layer are trained with given activation functions and initial values of weight vectors successively and individually. The hidden layers are trained using the autoencoder method, which is trying to make the output of each autoencoder as close to its input as possible. The beginning input vector for training serves as the input of the first hidden layer and the feature vector obtained by each hidden layer serves as the input of next hidden layer. In the end, the output layer is trained using the feature vector obtained by the last hidden layer and the targeted output vector in a supervised way. After all hidden layers and the output layer being trained step by step individually, the whole structure of DNN model could be formed by cascading input layer, first half part of each autoencoder and the eventual output layer. Then, prepared input data and targeted output data for training are used together to train the whole DNN model applying the back-propagation (BP) algorithm in a supervised way, which is referred to as fine-tuning. After this, the testing stage has been completed and the DNN model is ready for testing, which means that the DNN model has learned to represent the nonlinear relation between the output and the input. Afterwards, in the testing stage, experimentally obtained data are input into the DNN model and the output will be obtained quickly by processing using the well trained DNN model.

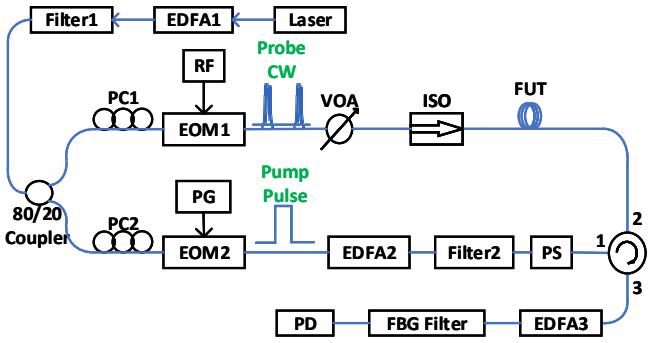

Fig. 2. BOTDA experiment setup, EDFA: erbium-doped fiber amplifier, PC: polarization controller, EOM: electro-optic modulator, RF: radio frequency, PG: pattern generator, VOA: variable optical attenuator, ISO: isolator, FUT: fiber under test, PS: polarization scrambler, FBG: fiber Bragg grating, PD: photodetector.

In our case, ideal BGS and T pairs are used as the training input and output data in the training stage. The number of components of each input vector is determined by the frequency sweeping range and step of the BOTDA experiment system and the output layer only contains just one neuron which is the temperature information we need. And in the testing stage, experimentally measured noisy BGS data along the fiber are input and the temperature information will be obtained using the DNN model as the output data.

B. Experiment Setup of our BOTDA System

We use the BOTDA experiment system shown as Fig. 2. The continuous wave (CW) light tunable laser is working at 1550 nm. Its output light is amplified by the EDFA1 and filtered by the filter1 and then splits into two branches using an 80/20 coupler. The light at the upper branch is modulated by EOM1 biased at null point to suppress the optical carrier and driven by an RF around BFS. A VOA is used to control the probe light power before entering the FUT and an isolator is used to block the light entering in reverse direction. At the lower branch, the CW light is modulated by the EOM2 with a pattern generator to generate 20 ns pump pulse which corresponds to 2 m spatial resolution of this system. The EDFA2 is used to amplify the peak power of the pump pulse and the filter2 is used to remove the amplified spontaneous emission (ASE) noise brought by EDFA2. In addition, a polarization scrambler is used to suppress the polarization dependent noise since the stimulated Brillouin scattering (SBS) effect is sensitive to polarization. The CW probe and pump pulse are counter propagating and interacting under SBS in the FUT. Then the CW probe signal is filtered using a FBG and detected by a 125 MHz photodetector. The local BGS along the FUT for processing is obtained by sweeping the frequency of probe light around the BFS.

III. Result and Disccusion

Before using DNN for temperature extraction, the linear BFS-temperature relationship is measured experimentally and the corresponding coefficient is found to be 0.974968 MHz/°C, as shown in Fig. 3. We use this BFS-temperature relationship and theoretical Lorentz curve to obtain data for DNN training with ideal BGS as input and corresponding temperature as

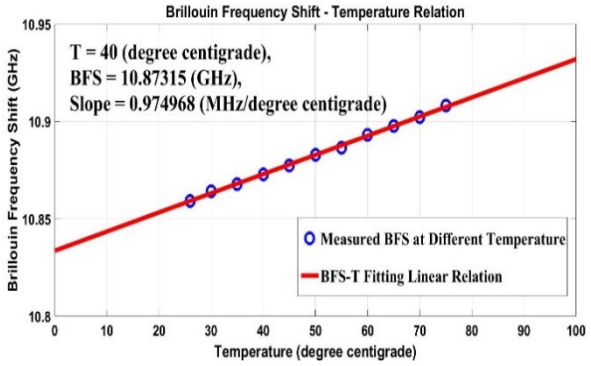

Fig. 3. The measured Brillouin frequency shift at different temperature and the fitting linear relation between them.

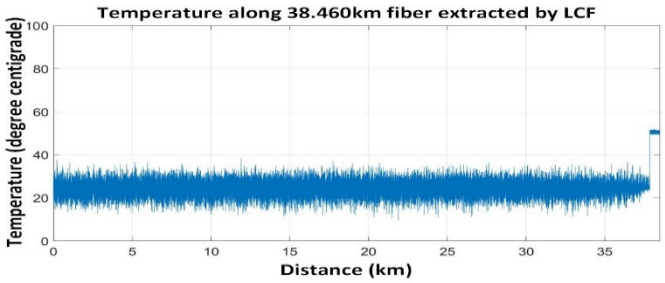

Fig. 4. Temperature distribution along the whole 38.460 km FUT with last 607 m fiber heated to 50 degrees centigrade extracted by LCF.

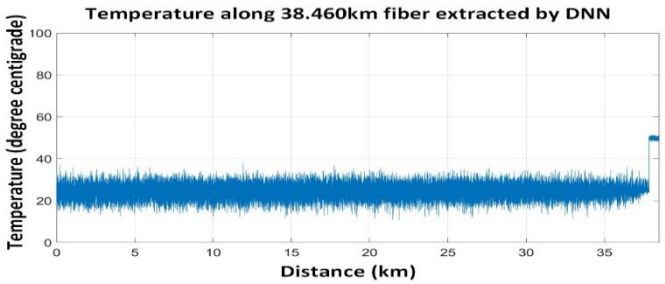

Fig. 5. Temperature distribution along the whole 38.460 km FUT with last 607 m fiber heated to 50 degrees centigrade extracted by DNN.

targeted output. In the construction of training data, the temperature range is from 0 to 100 °C and the BGS under each temperature has a linewidth ranging from 40 to 70 MHz at a step of 1 MHz, so the DNN could be used for practical measurement where the linewidth has variations. The temperature step is chosen to be 0.1 °C which is enough for training. Therefore, we have 31031 ideal BGS- temperature pairs for DNN training. The frequency sweeping range from 10.760 to 11.010 GHz with frequency step of 1 MHz. So, each input vector of our DNN model should contain 251 components, which means that we have 251 neurons in the input layer of DNN model. Since there is no specific guideline about how many hidden layers should be adopted and how many neurons should be contained in each hidden layer, the optimization process of DNN structure is a processing of try and error. The finalized DNN model structure contains 2 hidden layers because it is enough for acceptable performance

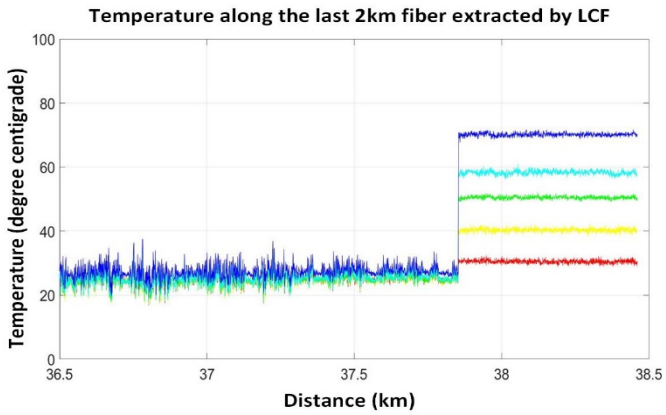

Fig. 6. The temperature distribution information in the last 2 kilometer fiber extracted by LCF.

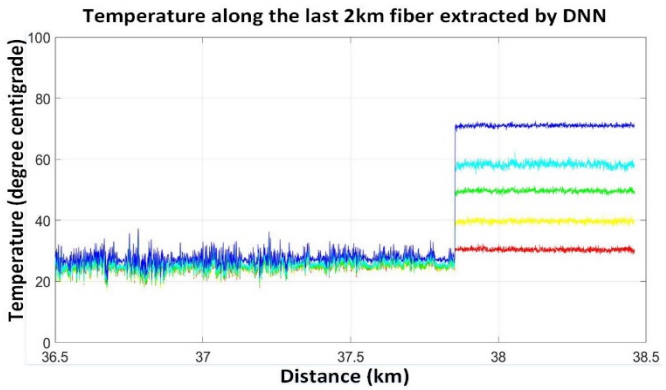

Fig. 7. The temperature distribution information in the last 2 kilometer fiber extracted by DNN.

TABLE I. ERROR PERFORMANCE COMPARISON OF DNN AND LCF IN LAST 607 METER HEATED FIBER.

Performance / Temperature	RMSE[a]		SD[b]	
	LCF	*DNN*	*LCF*	*DNN*
30	0.7533	0.6998	0.5578	0.5467
40	0.7015	0.6733	0.6172	0.6094
50	0.6769	0.6311	0.4683	0.5314
60	1.8465	1.9660	0.7354	0.9673
70	0.7387	1.2976	0.7234	0.7917

[a] Root mean square error, [b] Standard deviation.

and more number of hidden layers will bring much longer training time which increases exponentially with the number of hidden layers. And the number of neurons in the first hidden layer and the second hidden layer are determined to be 50 and 10 respectively after different trials.

After the training of the DNN model, the measured local BGS data along 38.460 km FUT with last 607 m heated to different temperatures are sent to the input layer of the DNN model. The temperature distributions along the whole FUT with last 607 meter fiber heated to 50 °C extracted by LCF and DNN are shown in Fig. 4 and Fig. 5, respectively.

Moreover, we also compare the results using DNN when the last fiber section heated to 30, 40, 50, 60 and 70 °C with those using conventional LCF. The extracted temperature information in the last 2 km FUT using LCF method and DNN method are shown in Fig. 6 and Fig. 7, respectively. We can see that the temperature distribution extracted by DNN is as good as that by LCF method. To show the comparison clearly, specific error performance including root-mean-square error (RMSE) and standard deviation (SD) calculated with the last 607 m heated fiber section are shown in Table 1, for both LCF and DNN. From Table 1 we could see that the error performance of temperature extraction using LCF method and that of using DNN are quite similar. In the future, better performance of using DNN to extract temperature distribution is expected to be obtain by increasing the extent of training and optimizing the structure of DNN.

IV. Conclusion

We have demonstrated the extraction of temperature distribution information along the 38.46 km FUT using the DNN method in our BOTDA temperature sensing system. We have compared the performance of DNN and LCF methods. The results show that the DNN can be used to extract the temperature with comparable accuracy to conventional LCF method. Moreover, it has the advantage of reducing the processing time significantly. Work of optimizing the DNN model to discover other advantages and obtain better accuracy for temperature extraction in BOTDA system will be researched in the future.

Acknowledgment

The authors would like to thank the financial supports from the HKPU grant 1-ZVHA and the Project of Strategic Importance 1-ZVGB.

References

[1] T. Horiguchi and M. Tateda, "BOTDA-nondestructive measurement of single-mode optical fiber attenuation characteristics using Brillouin interaction: theory," Journal of Lightwave Technology, vol. 7, no. 8, pp. 1170-1176, 1989.

[2] X. Bao and L. Chen, "Recent progress in Brillouin scattering based fiber sensors." Sensors, vol. 11, no. 12, pp. 4152-4187, 2011.

[3] Y. Dong, D. Ba, T. Jiang, D. Zhou, H. Zhang, C. Zhu, Z. Lu, H. Li, L. Chen and X. Bao, "High-spatial-resolution fast BOTDA for dynamic strain measurement based on differential double-pulse and second-order sideband of modulation," IEEE Photonics Journal, vol. 5, no. 3, pp. 2600407-2600407, 2013.

[4] A. Denisov, M. Soto and L. Thévenaz, "Going beyond 1000000 resolved points in a Brillouin distributed fiber sensor: theoretical analysis and experimental demonstration," Light: Science & Applications, vol. 5, no. 5, p. e16074, 2016.

[5] M. Soto, X. Angulo-Vinuesa, S. Martin-Lopez, S. Chin, J. Ania-Castanon, P. Corredera, E. Rochat, M. Gonzalez-Herraez and L. Thevenaz, "Extending the real remoteness of long-range Brillouin optical time-domain fiber analyzers," Journal of Lightwave Technology, vol. 32, no. 1, pp. 152-162, 2014.

[6] J. Mompó, J. Urricelqui and A. Loayssa, "Brillouin optical time-domain analysis sensor with pump pulse amplification," Optics Express, vol. 24, no. 12, p. 12672, 2016.

[7] R. Ruiz-Lombera, J. Urricelqui, M. Sagues, J. Mirapeix, J. Lopez-Higuera and A. Loayssa, "Overcoming nonlocal effects and Brillouin threshold limitations in Brillouin optical time-domain sensors," IEEE Photonics Journal, vol. 7, no. 6, pp. 1-9, 2015.

[8] Deng, Li, G. Hinton, and B. Kingsbury. "New types of deep neural network learning for speech recognition and related applications: An overview," 2013 IEEE International Conference on Acoustics, Speech and Signal Processing, 2013.

[9] G. Hinton, L. Deng, D. Yu, G. Dahl, A. Mohamed, N. Jaitly, A. Senior, V. Vanhoucke, P. Nguyen, T. Sainath and B. Kingsbury, "Deep neural networks for acoustic modeling in speech recognition: the shared views of four research groups," IEEE Signal Processing Magazine, vol. 29, no. 6, pp. 82-97, 2012.

[10] G. Dahl, D. Y. L. Deng and A. Acero, "Context-dependent pre-trained deep neural networks for large-vocabulary speech recognition," IEEE Transactions on Audio, Speech, and Language Processing, vol. 20, no. 1, pp. 30-42, 2012.

[11] F. Khan, K. Zhong, W. Al-Arashi, C. Yu, C. Lu and A. Lau, "Modulation format identification in coherent receivers using deep machine learning," IEEE Photonics Technology Letters, vol. 28, no. 17, pp. 1886-1889, 2016.

[12] A. Azad, L. Wang, N. Guo, H. Tam and C. Lu, "Signal processing using artificial neural network for BOTDA sensor system," Optics Express, vol. 24, no. 6, p. 6769, 2016.